Proceedings of
The Fourth National Congress on Fluids Engineering
August 23-25, 2006, Kyungju, Korea

Direct numerical simulation of the turbulent boundary layer with rod-roughened wall

Seung-Hyun Lee* and Hyung Jin Sung**

표면조도가 있는 난류경계층에서의 직접수치모사

이승현* · 성형진**

Keywords : *Surface Roughness(표면조도), Direct Numerical Simulation(직접수치모사), Turbulent Boundary Layer(난류경계층)*

Abstract

The effects of surface roughness on a spatially-developing turbulent boundary layer (TBL) were investigated by performing direct numerical simulations of TBLs over rough and smooth walls. The Reynolds number based on the momentum thickness was varied in the range Re_θ=300~1400. The roughness elements used were periodically arranged two-dimensional spanwise rods, and the roughness height was $k=1.5\theta_{in}$, which corresponds to k/δ=0.045~0.125. To avoid generating a rough wall inflow, which is prohibitively difficult, a step change from smooth to rough was placed $80\theta_{in}$ downstream from the inlet. The spatially-developing characteristics of the rough-wall TBL were examined. Along the streamwise direction, the friction velocity approached a constant value and a self-preserving form of the turbulent stress was obtained. Introduction of the roughness elements affected the turbulent stress not only in the roughness sublayer but also in the outer layer. Despite the roughness-induced increase of the turbulent stress in the outer layer, the roughness had only a relatively small effect on the anisotropic Reynolds stress tensor in the outer layer. Inspection of the triple products of the velocity fluctuations revealed that introducing the roughness elements onto the smooth wall had a marked effect on vertical turbulent transport across the whole TBL. By contrast, good surface similarity in the outer layer was obtained for the third-order moments of the velocity fluctuations.

1. Introduction

In real engineering applications involving wall-bounded boundary layer flow (e.g. automobiles, ships, airplanes, heat-exchangers, and weather prediction), the roughness of the wall surface is an important design parameter because it influences characteristics such as the transport of heat, mass and momentum. Although the effects of surface roughness on a TBL have been examined in many experimental and numerical studies, knowledge of these effects remains incomplete. Previous studies on the effect of surface roughness on a TBL are well reviewed by Raupach et al. [1] and Jimenez [2]. These reviews support the wall similarity hypothesis of Townsend [3], which states that outside the roughness sublayer turbulent motions are independent of the surface roughness and that the interaction between the inner and outer layers is very weak at sufficiently large Reynolds numbers. In further support of this similarity hypothesis, Flack et al. [4] and Connelly et al. [5] recently observed that the outer layers of flows past smooth and rough walls were similar in terms of both mean flow and turbulent statistics. However, results from several experimental studies have been contrary to the similarity hypothesis [6-10].

Recently, several numerical studies using DNS (Direct Numerical Simulation) and LES (Large Eddy Simulation) have been conducted on turbulent channel flow with a rough wall [11-14]. Krogstad et al. [15] compared the experimental results of Bakken et al. [16] for turbulent flow in a symmetric channel with a rod-roughness of k/h=0.034 with the results obtained by Ashrafian et al. [12] in a DNS of the same system. They observed good agreement between the experimental and simulation results, with both showing no significant difference between the characteristics of the outer layer in the smooth walled system and those in the rough walled system. And they conjectured that the degree to which surface roughness affects the outer layer is influenced by the flow type, for example symmetric channel flow, asymmetric channel flow, boundary layer, and so on.

Despite the fact that most experimental studies have examined the characteristics of TBLs, the majority of numerical studies (LES and DNS) have examined turbulent channel flows. This discrepancy can be attributed to the difficulty of simulating TBLs. A TBL is a spatially developing flow, and hence periodic boundary conditions along the streamwise direction are not applicable. Moreover, realistic turbulent inflows must be generated at the inlet and the domain size along the downstream direction must be sufficiently large to reach a new rough-wall equilibrium state after the roughness step change. And a very fine grid spacing must be used along the streamwise and wall-normal directions to simulate systems with a very small ratio of roughness height ratio of roughness height to boundary layer. These difficulties mean that DNS is computationally very expensive and complex. For these reasons, no DNSs of a rough-wall TBL have been performed, and the absence of DNS data for these systems has made it difficult to validate experiments on rough-wall TBLs.

In the present study, we carried out DNSs of TBLs with rough and smooth walls and compared our findings with previous experimental data. The objective of the present study was to elucidate the interaction between the inner and outer layers arising from the roughness and to delineate the basic characteristics of a rough-wall TBL.

* 한국과학기술원 기계공학과, leehuiso@kaist.ac.kr
** 한국과학기술원 기계공학과, hjsung@kaist.ac.kr

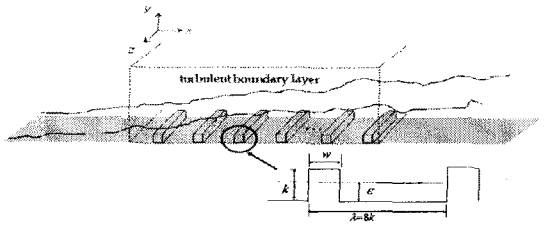

Fig. 1 Schmatic diagrams of computational domain and rod roughness.

2. Numerical details

The governing equations are incompressible Navier-Stokes equations and continuity equation and they were solved with a fully implicit fractional-step method proposed by Kim et al. [17]. The roughness was numerically treated by the immersed boundary method of Kim et al. [18]. As shown in Fig. 1, the domain size was $768\theta_{in}\times60\theta_{in}\times80\theta_{in}$ for rough wall and $1536\theta_{in}\times60\theta_{in}\times80\theta_{in}$ for smooth wall in the streamwise, wall-normal and spanwise directions, where the corresponding mesh number is 2049×150×257 for rough and smooth walls. The domain size in the streamwise direction was sufficiently long that the effects of the surface roughness step change could be neglected. Realistic velocity fluctuations at the inlet were provided based on the method of Lund et al. [19].

The Reynolds number based on the momentum thickness at the inlet for both cases was Re_θ=300. The convective outflow condition was used at the exit and the no-slip boundary condition was imposed at the solid wall. At the free-stream, the conditions $u= U\infty$ and $\partial v/\partial y=\partial w/\partial y=0$ were imposed. Periodic boundary conditions were used in the spanwise direction. The roughness takes the form of two-dimensional spanwise rods with a squre cross-section that are periodically arranged in the streamwise direction with a pitch of is $\lambda=8k$. The roughness height is $k=1.5\theta_{in}$, which corresponds to $k/\delta=0.045\sim0.125$ and $k^+=32\sim45$. The first rod is placed at $80\theta_{in}$ downstream from the inlet, the surface condition therefore changes abruptly from smooth to rough at this location, which is defined as x=0.

The friction velocity is obtained using spatially-averaged skin frictional drag and form drag similar as the method of Leonardi et al. [13]. The friction velocity of the rough wall abruptly increases just upstream of the step change in the roughness and decreases slowy, converging to a constant value at about $x>300\theta in$. The distance (ϵ) from the bottom wall to the virtual origin is considered as the centroid of the moment of forces acting on the roughness elements [20]. The variation of ϵ along the downstream direction is very small and ϵ is about half of k. In the present DNSs, $y'=y-\epsilon$ is defined as the distance from the virtual origin.

3. Results

3.1 Self-preserving form for rough wall

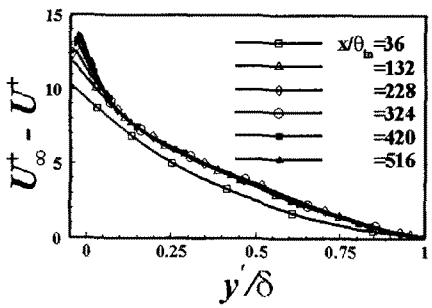

Fig. 2 Variations of streamwise mean velocity along the downstream.

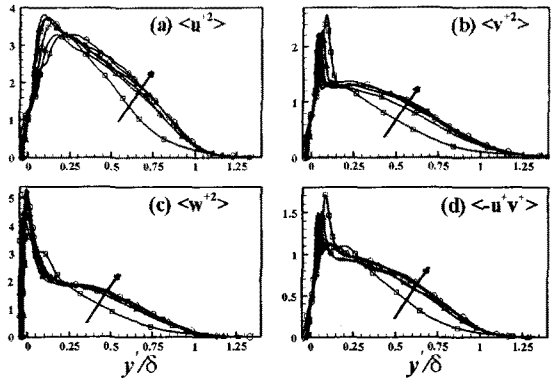

Fig. 3 Variations of turbulent Reynolds stresses along downstream in the outer coordinates. Symbols in Fig. 2.

After the roughness step change, there is a transient region in which the flow adapts to the new boundary conditions and the domain size along the streamwise direction should be large to reach a new equilibrium state where a self-preservation form is achieved. The velocity defect profiles at various locations along the streamwise direction are shown in Fig. 2. For $x>132\theta in$, the velocity defect profiles become almost identical, indicating that self-preservation has been established. Fig. 3 shows the variations of the Reynolds stress in the outer layers along the streamwise direction, which are normalized by the outer length scale. y'/δ. the Reynolds stresses in the outer layer increase with moving downstream. This increase can be attributed to the presence of the roughness step change, which causes a large increase in turbulent fluctuations near the wall that then propagate to the outer layer as the flow moves downstream. Self-preservation is obtained in the outer layer after $x=324\theta in$ when normalized by the boundary layer thickness as the outer length scale.

3.2 Roguhness sublayer

Introduction of the rod roughness elements onto the smooth surface significantly affects the turbulent flow structures, leading to very high turbulent intensities in the vicinity of the wall. This near-wall region, which is known as the roughness sublayer, is generally assumed to have a height of 2~5 times the roughness height. The limit of the roughness sublayer is defined as the point at which the turbulence statistics become spatially homogeneous [14]. Fig. 4 shows that the profiles of all flow quantities at different locations (I)~(IV) are indistinguishable above y=5k. These results indicate that the roughness sublayer is located in the region y<5k and the outer layer region is above y=5k.

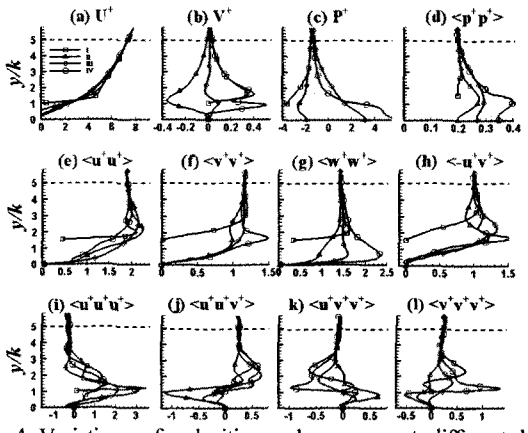

Fig. 4 Variations of velocities and pressure at different locations (I)~(IV) in the roughness sublayer.

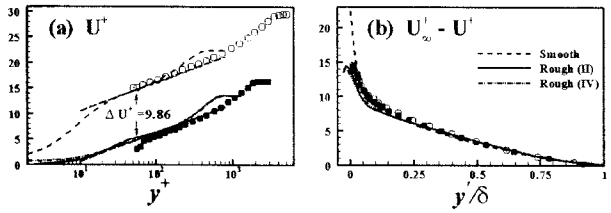

Fig. 5 Mean velocity profiles. (a) inner variables; (b) velocity defect forms, (○) smooth wall, (●) rod roughness (Krogstad et al. [8]).

3.3 Mean velocity and Reynolds stresses

The mean streamwise velocity profiles for smooth and rough walls are shown in Figure 12. The general mean velocity shift (ΔU^+) is clearly shown and is estimated to be 9.86. The effect sand grain roughness height is k_s= 211.5, which corresponds to strong roughness according to the classification of Flack et al. [4]. The ratio k_s/k is 6.39, which is similar to that of the rod roughness of Krogstad et al. [8]. The velocity defect profiles, displayed in Figure 12 (b), show very good agreement between the present DNS results and the experimental data of Krogstad et al. [8]. In the outer layer, the velocity defect profiles of the smooth and rough walls collapse well and show good surface similarity.

The Reynolds stresses normalized by u_τ^2 are compared in Fig. 6 for the smooth and rough walls. In the outer layer, the $\langle u^{+2}\rangle$ for the rough wall system becomes greater than that of the smooth wall system. These trends are in good agreement with the experimental data of Krogstad et al. [8]. The wall-normal stresses $\langle v^{+2}\rangle$, by contrast, are higher in the rough than in the smooth wall system in both the roughness sublayer and in the outer layer, although the increase of $\langle v^{+2}\rangle$ in the outer layer is smaller than that observed by Krogstad et al. [8]. The spanwise normal stresses $\langle w^{+2}\rangle$ and Reynolds shear stresses $\langle -u^+v^+\rangle$ exhibit a similar increase in the outer layer. The present results are in good agreement with the experimental data of Krogstad et al. (1999) and Keirsbulck et al. (2002). Consistent with the findings of these experiments, our results indicate that the introduction of surface roughness affects the turbulent Reynolds stresses outside the roughness sublayer.

3.4 Reynolds stress aniostropy

The profiles of the Reynolds anisotropy tensors b_{ij}, displayed in Fig. 7, show that the introduction of rod roughness significantly reduces the anisotropy within the roughness sublayer. In particular, the decrease of b_{11} and increase of b_{22} and b_{33} are prominent near the leading edge in the roughness sublayer. The increase of b_{33} in the cavity between consecutive rods is markedly stronger than that of b_{22}, indicating that

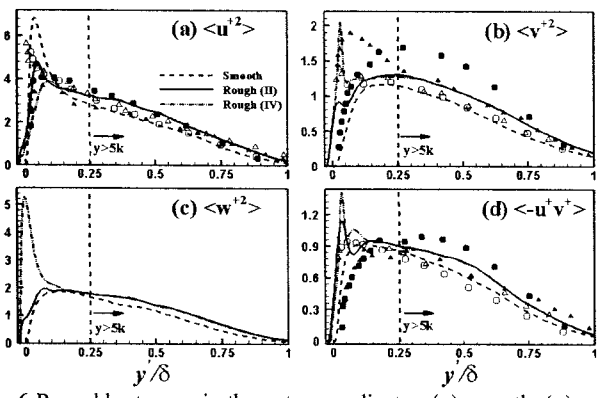

Fig. 6 Reynolds stresses in the outer coordinates. (○) smooth, (●) rod (Krogstad et al. [8]); (△) smooth, (▲) rod (Keirsbulck et al. [9])

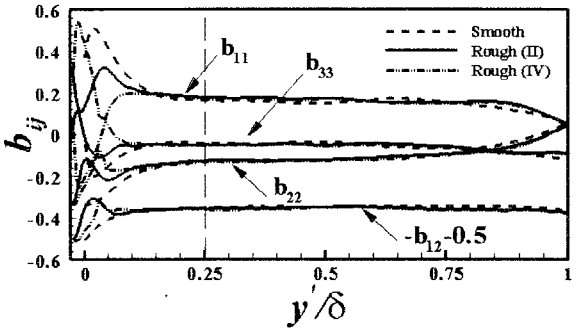

Fig. 7 Anisotropy tensors in the outer coordinates.

most of the turbulent energy of the streamwise component is transformed into that of the spanwise component in the cavity due to the blockage effect of the rod roughness. In the outer layer, the introduction of surface roughness has little effect on the Reynolds anisotropy tensor. This finding differs from most previous experimental results, but is similar to the behavior observed in a turbulent channel flow [15]. The Reynolds stress anisotropy tensors show good surface similarity in the outer layer. Although the increased production of turbulent kinetic energy in the vicinity of the rough wall causes an increase in the Reynolds stresses, no significant contribution is made to the ratio of each Reynolds stress component. This suggests that the turbulent kinetic energy is redistributed from $\langle u^{+2}\rangle$ to $\langle v^{+2}\rangle$ and $\langle w^{+2}\rangle$ in the roughness sublayer rather than in the outer layer.

3.5 Third-order turbulence statistics

Fig. 8 (a)~(d) show profiles of the velocity triple products of fluctuating components $\langle u^{+3}\rangle$, $\langle u^{+2}v^+\rangle$, $\langle u^+v^{+2}\rangle$ and $\langle v^{+3}\rangle$, normalized by u_τ^3, for smooth and rough walls. The present rough-wall DNS data for $\langle u^{+3}\rangle$ differ only slightly from the smooth-wall data in the region of $y/\delta>0.25$, but differ markedly in the region of $y/\delta<0.25$. For the rough wall, the positive peak of $\langle u^{+3}\rangle$ near the wall is less intense and moves outwards, and the negative peak disappears. For the smooth wall, <u+3> changes from positive to negative at about $y/\delta=0.03$ ($y^+\approx13.5$), whereas for the rough wall this sign change occurs farther from the wall, at $y/\delta=0.1\sim0.14$ ($y^+\approx68\sim92$), indicating that sweep motions ($u'>0$, $v'<0$) are stronger near the rough wall than the smooth wall. This may be due to the less strict wall-normal boundary condition for the rough wall, which would allow a greater amount of high-momentum fluid to be swept into the cavity between the rods.). For the rough wall, $\langle v^{+3}\rangle$ has a negative peak in the cavity by the increased sweep events towards the cavity. Outside the cavity (y>k), $\langle v^{+3}\rangle$ is positive and wall-normal

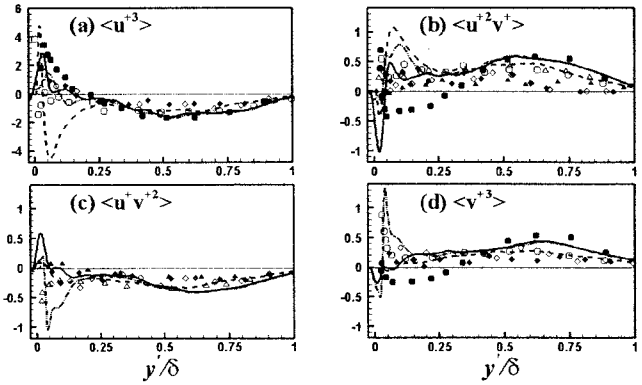

Fig. 8 Velocity triple products in the outer coordinates. (◇) smooth, (◆) rod (Bandyopadhyay et al. [6]); (○) smooth, (●) rod (Krogstad et al. [8]); (△) smooth, (▲) rod (Keirsbulck et al. [9])

velocity fluctuations are transported outward from the wall, indicating that ejection events are very strong above the leading edge. In the outer layer, the slope of $\langle u^{+2}v^{+}\rangle$ for the rough wall is positive and larger than that of the smooth wall in the region of $0.25<y/\delta<0.64$, and the sign changes at $y/\delta\approx0.64$. In the profiles of $\langle u^{+}v^{+2}\rangle$ and $\langle v^{+3}\rangle$, the slope is increased in the same region. This indicates that there is a loss of kinetic energy due to transport of this energy away from the wall and that the loss is larger for the rough wall than for the smooth wall. This is consistent with the experimental results of Krogstad et al. [8] for TBL. The data for turbulent channel flow with smooth and rough walls showed that there was only a gain in the kinetic energy transported from the wall, with no change in the sign of the slope [16, 21]. These different characteristics of the transport mechanism in the outer layer between boundary layer and channel flow may be related to different effects of surface roughness on Reynolds turbulent stresses in the outer layer.

4. Conclusions

In the present study we sought to elucidate the effects of surface roughness on a TBL over a wall. To determine the basic information on the rough-wall TBL, we performed DNSs of the TBLs over rough and smooth walls and compared the results with previous experimental data. Emphasis was placed on the interaction between the inner and outer layers induced by the surface roughness. Near the region where the surface changed from smooth to rough, the surface roughness significantly affected the turbulence statistics due to blockage of the flow by the first upstanding rod. After the step change region, self-preservation of the Reynolds stresses was achieved after $x=324\theta_{in}$. In the rough wall simulations, the domain size along the streamwise direction was sufficiently long for the flow to reach a new equilibrium state above the rough wall. The mean velocity defect form showed very good surface similarity in the outer layer. However, the turbulent Reynolds stresses of the rough-wall flow differed from those of the smooth wall flow not only inside the roughness sublayer, but also outside. By contrast, the Reynolds stress anisotropy tensor showed good surface similarity in the outer layer, indicating no significant contribution is made to the ratio of each Reynolds stress component. In the region of the outer layer adjoining the roughness sublayer, the triple products of velocity fluctuations for the rough wall were stronger than those for the smooth wall. Increased sweep events were observed near the focal points of two recirculation regions in the cavity. Outside the cavity (y>k), the wall-normal velocity fluctuations were transported outward from the wall and ejection events were very strong above the leading edge. Strong transport of $\langle u^{+2}\rangle$ and $\langle -u^{+}v^{+}\rangle$ were strongly related to these increased sweep and ejection events. In the outer layer, a loss of kinetic energy occurred, which was transported away from the wall. The transport mechanism of TBL in the outer layer was different from that of channel flow and it may be related with different effects of roughness in the outer layer.

Acknowledgement

This work was supported by the Basic Research Program (R01-2004-000-10521-0) of the Korea Science & Engineering Foundation and partially supported by the Grand Challenge Supercomputing Program of the Korea Institute of Science and Technology Information with Dr. Lee and Ali as the technical supporter.

References

[1] Raupach, M. R., Antonia, R. A. and Rajagopalan, S., 1991, "Rough-wall Turbulent Boundary Layers," Appl. Mech. Rev., Vol. 44, pp. 1-25.

[2] Jimenez, J., 2004, "Turbulent Flows over Rough Walls," Annu. Rev. Fluid Mech., Vol. 36, pp. 173-196.

[3] Townsend, A. A., 1976, "The Structure of Turbulent Shear Flow," Cambridge University Press, Cambridge.

[4] Flack, K. A., Schultz, M. P. and Shapiro, T. A., 2005, "Experimental Support for Townsend's Reynolds Number Similarity," Phys. Fluids, Vol. 17, published online.

[5] Connelly, J. S., Schultz, M. P. and Flack, K. A., 2005, "Velocity-defect Scaling for Turbulent Boundary Layers with a Range of Relative Roughness," Exp. Fluids, Vol. 40, pp. 188-195.

[6] Bandyopadhyay, P. R. and Watson, R. D., 1988, "Structure of Rough-wall Boundary Layers," Phys. Fluids, Vol. 31, pp. 1877-1883.

[7] Krogstad, P. -Å., Antonia, R. A. and Browne, L. W. B., 1992, "Comparison between Rough- and Smooth-wall Turbulent Boundary Layers," J. Fluid Mechanicsm Vol. 245, pp. 599-617.

[8] Krogstad, P. -Å. and Antonia, R. A., 1999, "Surface Roughness Effects in Turbulent Boundary Layers," Exp. Fluids, Vol. 27, pp. 450~460.

[9] Keirsbulck, L., Labraga, L., Mazouz, A. and Tournier, C., 2002, "Surface Roughness Effects on Turbulent Boundary Layer Structures," J. Fluids Engineering, Vol. 124, pp. 127-135.

[10] Smalley, R. J., Leonardi, S., Antonia, R. A., Djenidi, L. and Orlandi, P., 2002, "Reynolds Stress Anisotropy of Turbulent Rough Wall Layers," Exp. Fluids, Vol. 33, pp. 32-37.

[11] Lee, C., 2002, "Large-eddy Simulation of Rough-wall Turbulent Boundary Layers," AIAA J., Vol. 40, pp. 2127-2130.

[12] Ashrafian, A., Andersson, H. I. and Manhart, M., 2004, "DNS of Turbulent Flow in a Rod-roughened Channel," Int. J. Heat and Fluid Flow, Vol. 25, pp. 373-383.

[13] Leonardi, S., Orlandi, P., Smalley, R.J., Djenidi, L. and Antonia, R.A., 2003, "Direct Numerical Simulations of Turbulent Channel Flow with Transverse Square Bars on One Wall," J. Fluid Mechanics, Vol. 491, pp. 229-238.

[14] Bhaganagar, K., Kim, J. and Coleman, G., 2004, "Effect of Roughness on Wall-bounded Turbulence," Flow, Turbulence and Combustion, Vol. 72, pp. 463-492.

[15] Krogstad, P. –Å., Andersson, H. I., Bakken, O. M. and Ashrafian, A., 2005, "An Experimental and Numerical Study of Channel flow with Rough Walls," J. Fluid Mechanics, Vol. 530, pp. 327-352.

[16] Bakken, O. M. and Krogstad, P. –Å, 2005, "Reynolds Number Effects in the Outer Layer of the Turbulent Flow in a Channel with Rough Walls," Phys. Fluids, Vol. 17, published online.

[17] Kim, K., Baek, S.-j. and Sung, H. J., 2002, "An Implicit Velocity Decoupling Procedure for the Incompressible Navier-Stokes Equations," Int. J. Numer. Meth. Fluids, Vol. 38, pp. 125-138.

[18] Kim, J., Kim, D. and Choi, H., 2001, "An Immersed Boundary Finite-volume Method for Simulations of Flow in Complex Geometries," J. Computational Physics, Vol. 171, pp. 132-150.

[19] Lund, T. S., Wu, X. and Squires, K. D., 1998, "Generation of Turbulent Inflow Data for Spatially-developing Boundary Layer Simulation," J. Computational Physics. Vol. 140, pp. 233-258.

[20] Jackson, P. S., 1981, "On the Displacement Height in the Logarithmic Profiles," J. Fluid Mechanics, Vol. 111, pp. 15-25.

[21] Ashrafian, A. and Andersson, H. I., 2006, "The Structure of Turbulence in a Rod-roughened Channel," Int. J. Heat and Fluid Flow, Vol. 27, pp. 65-79.